





## Article

# Bernardevansite, $\text{Al}_2(\text{Se}^{4+}\text{O}_3)_3 \cdot 6\text{H}_2\text{O}$ , dimorphous with alfredopetrovite and the Al-analogue of mandarinoite, from the El Dragón mine, Potosí, Bolivia

Hexiong Yang<sup>1\*</sup> , Xiangping Gu<sup>2</sup> , Robert A. Jenkins<sup>1</sup>, Ronald B. Gibbs<sup>1</sup> and Robert T. Downs<sup>1</sup>

<sup>1</sup>Department of Geosciences, University of Arizona, 1040 E. 4<sup>th</sup> Street, Tucson, AZ 85721-0077, USA; and <sup>2</sup>School of Geosciences and Info-Physics, Central South University, Changsha, Hunan 410083, China

### Abstract

A new mineral species, bernardevansite (IMA2022-057), ideally  $\text{Al}_2(\text{Se}^{4+}\text{O}_3)_3 \cdot 6\text{H}_2\text{O}$ , has been discovered from the El Dragón mine, Potosí Department, Bolivia. It occurs as aggregates or spheres of radiating bladed crystals on a matrix consisting of Co-bearing krut'aite–penroseite. Associated minerals are Co-bearing krut'aite–penroseite, chalcomenite and 'clinochalcomenite'. Bernardevansite is colourless in transmitted light, transparent with white streak and vitreous lustre. It is brittle and has a Mohs hardness of 2½–3. Cleavage is not observed. The measured and calculated densities are 2.93(5) and 2.997 g/cm<sup>3</sup>, respectively. Optically, bernardevansite is biaxial (+), with  $\alpha = 1.642(5)$ ,  $\beta = 1.686(5)$  and  $\gamma = 1.74(1)$  (white light). An electron microprobe analysis yielded an empirical formula (based on 15 O apfu)  $(\text{Al}_{1.26}\text{Fe}_{0.82})_{\Sigma 2.08}(\text{Se}_{0.98}\text{O}_3)_3 \cdot 6\text{H}_2\text{O}$ , which can be simplified to  $(\text{Al},\text{Fe}^{3+})_2(\text{SeO}_3)_3 \cdot 6\text{H}_2\text{O}$ .

Bernardevansite is the Al-analogue of mandarinoite,  $\text{Fe}_2^{3+}(\text{SeO}_3)_3 \cdot 6\text{H}_2\text{O}$  or dimorphous with  $P6_2c$  alfredopetrovite. It is monoclinic, with space group  $P2_1/c$  and unit-cell parameters  $a = 16.5016(5)$ ,  $b = 7.7703(2)$ ,  $c = 9.8524(3)$  Å,  $\beta = 98.258(3)^\circ$ ,  $V = 1250.21(6)$  Å<sup>3</sup> and  $Z = 4$ . The crystal structure of bernardevansite consists of a corner-sharing framework of  $M^{3+}\text{O}_6$  ( $M = \text{Al}$  and  $\text{Fe}$ ) octahedra and  $\text{Se}^{4+}\text{O}_3$  trigonal pyramids, leaving large voids occupied by the  $\text{H}_2\text{O}$  groups. There are two unique  $M^{3+}$  positions:  $M1$  is octahedrally coordinated by  $(4\text{O} + 2\text{H}_2\text{O})$  and  $M2$  by  $(5\text{O} + \text{H}_2\text{O})$ . The structure refinement indicates that Al preferentially occupies  $M1$  ( $= 0.692\text{Al} + 0.308\text{Fe}$ ) over  $M2$  ( $= 0.516\text{Al} + 0.484\text{Fe}$ ). The substitution of the majority of Fe in mandarinoite by Al results in a significant reduction in its unit-cell volume from 1313.4 Å<sup>3</sup> to 1250.21(6) Å<sup>3</sup> for bernardevansite. The discovery of bernardevansite begs the question whether the  $\text{Fe}^{3+}$  end-member,  $\text{Fe}_2^{3+}(\text{SeO}_3)_3 \cdot 6\text{H}_2\text{O}$ , has two polymorphs as well, one with  $P2_1/c$  symmetry, as for mandarinoite and the other  $P6_2c$ , as for alfredopetrovite.

**Keywords:** bernardevansite, alfredopetrovite, mandarinoite, new mineral, crystal structure, Raman, El Dragón mine, Bolivia

(Received 17 November 2022; accepted 16 January 2023; Accepted Manuscript published online: 25 January 2023;

Associate Editor: Daniel Atencio)

### Introduction

Bernardevansite, ideally  $\text{Al}_2(\text{Se}^{4+}\text{O}_3)_3 \cdot 6\text{H}_2\text{O}$ , is a new mineral species from the El Dragón mine, Antonio Quijarro Province, Potosí Department, Bolivia. It is named in honour of Dr Bernard W. Evans (b. 1934, Fig. 1), an Emeritus Professor in Mineralogy and Petrology at the University of Washington in Seattle, Washington, USA. Bernard received his B.Sc. from the University of London King's College, England, 1955 and Ph.D. from the University of Oxford, England in 1959. He was an Assistant and Associate Professor at the University of California in Berkeley from 1965–1969 and a Professor at the University of Washington in Seattle from 1969–2001. Bernard's major research interests included petrology, mineralogy, geochemistry and

electron microprobe analysis, with outstanding contributions to the crystal chemistry and thermodynamics of amphiboles in particular and metamorphic minerals in general. In his over 50 years academic career, he has received numerous awards or honours, such as the Tennant Prize for Geology, King's College, London (1955), the Mineralogical Society of America (MSA) Award (1970), U.S. Senior Scientist Award, Humboldt Foundation (1988–89), the President of MSA (1993–94), Fulbright Scholar, France (1995–96) and the Roebing Medal of MSA (2008). Dr Evans has gladly accepted the proposed naming. The new mineral and its name (symbol Bev) have been approved by the Commission on New Minerals, Nomenclature and Classification (CNMNC) of the International Mineralogical Association (IMA2022-057, Yang *et al.*, 2023). The co-type samples have been deposited at the University of Arizona Alfie Norville Gem and Mineral Museum (Catalogue # 22712) and the RRUFF Project (deposition # R210010) (<http://rruff.info>). This paper describes the physical and chemical properties of bernardevansite, and its crystal structure determined from single-crystal X-ray

\*Author for correspondence: Hexiong Yang, Email: [hyang@arizona.edu](mailto:hyang@arizona.edu)

Cite this article: Yang H., Gu X., Jenkins R.A., Gibbs R.B. and Downs R.T. (2023) Bernardevansite,  $\text{Al}_2(\text{Se}^{4+}\text{O}_3)_3 \cdot 6\text{H}_2\text{O}$ , dimorphous with alfredopetrovite and the Al-analogue of mandarinoite, from the El Dragón mine, Potosí, Bolivia. *Mineralogical Magazine* 87, 407–414. <https://doi.org/10.1180/mgm.2023.7>

© University of Arizona, 2023. Published by Cambridge University Press on behalf of The Mineralogical Society of Great Britain and Ireland. This is an Open Access article, distributed under the terms of the Creative Commons Attribution licence (<http://creativecommons.org/licenses/by/4.0/>), which permits unrestricted re-use, distribution and reproduction, provided the original article is properly cited.



**Fig. 1.** A portrait of Dr Bernard W. Evans in 2008.

diffraction data, illustrating its structural relationships with mandarinoite and alfredopetrovite.

### Sample description and experimental methods

#### Occurrence

Bernardevansite was found on a specimen (Fig. 2) collected from the El Dragón mine (19°49'15"S, 65°55'00"W), Antonio Quijarro Province, Potosí Department, Bolivia. Associated minerals are

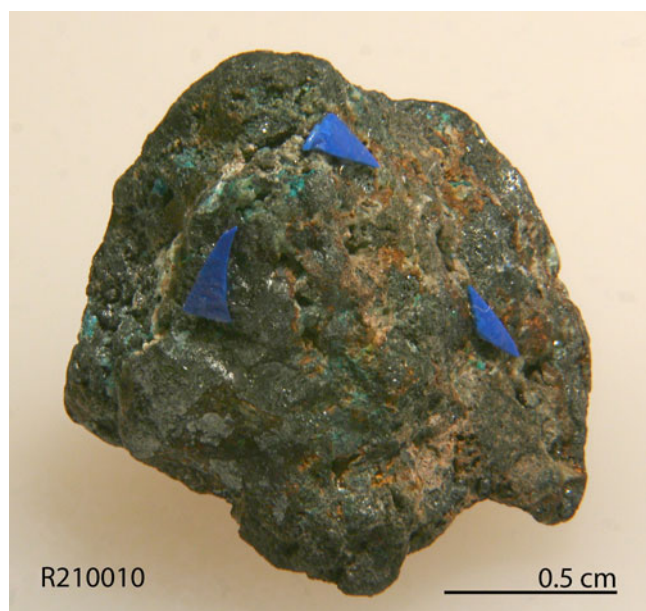


**Fig. 2.** The specimen on which the new mineral berneadevansite, indicated by the blue arrow, was found (R210010).

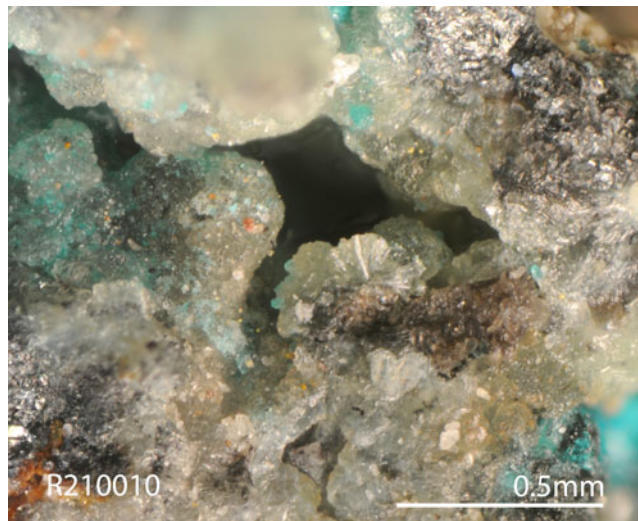


**Fig. 3.** A microscopic view of aggregates or spheres of pale grey to colourless, radiating bladed berneadevansite crystals (R210010).

Co-bearing krut'aite-penroseite (matrix), chalcocomenite and 'clin-ochalcocomenite' (not IMA-approved). Detailed descriptions on the geology and mineralogy of the El Dragón mine have been given by Grundmann *et al.* (1990, 2007) and Grundmann and Förster (2017). This mine exploited a telethermal deposit consisting of a single selenide vein hosted in sandstones and shales. The major ore mineral is krut'aite,  $\text{CuSe}_2$ , varying in composition to penroseite,  $\text{NiSe}_2$ . Later solutions rich in Bi, Pb and Hg resulted in the crystallisation of minerals such as clausenthalite, petrovicite, watkinsonite, and the recently described minerals eldragónite,  $\text{Cu}_6\text{BiSe}_4(\text{Se}_2)$  (Paar *et al.*, 2012), grundmannite,  $\text{CuBiSe}_2$  (Förster *et al.*, 2016), hansblockite,  $(\text{Cu,Hg})(\text{Bi,Pb})\text{Se}_2$  (Förster *et al.*, 2017), cerramojonite,  $\text{CuPbBiSe}_3$  (Förster *et al.*, 2018) and nickeltyrrellite,  $\text{CuNi}_2\text{Se}_4$  (Förster *et al.*, 2019). Oxidation produced a wide range of secondary Se-bearing minerals, such as favreauite,  $\text{PbBiCu}_6\text{O}_4(\text{SeO}_3)_4(\text{OH})\cdot\text{H}_2\text{O}$  (Mills *et al.*, 2014), alfredopetrovite,  $\text{Al}_2(\text{Se}^{4+}\text{O}_3)_3\cdot 6\text{H}_2\text{O}$  (Kampf *et al.*, 2016a), petermegawite  $\text{Al}_6(\text{Se}^{4+}\text{O}_3)_3[\text{SiO}_3(\text{OH})](\text{OH})_9\cdot 10\text{H}_2\text{O}$  (Yang *et al.*,



**Fig. 4.** A back-scattered electron image of aggregates of radiating bladed berneadevansite crystals (R210010).

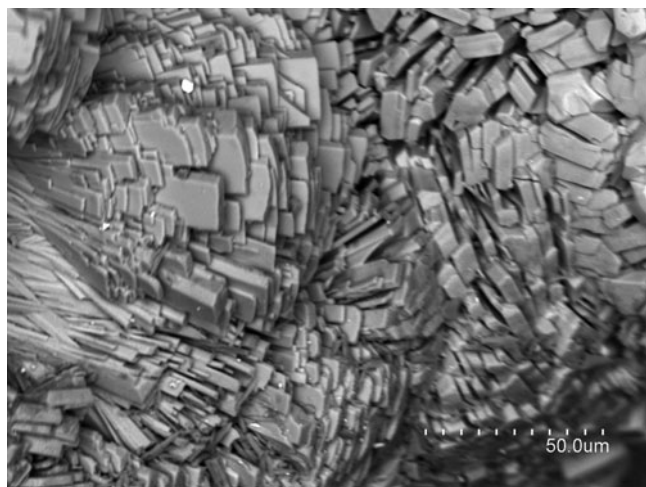


**Fig. 5.** A back-scattered electron image of aggregates of bladed bernardevansite crystals (R210010).

**Table 1.** Chemical compositions (in wt.%) of bernardevansite.\*

Constituent	Mean	Range	S.D.	Probe standard
Al <sub>2</sub> O <sub>3</sub>	11.38	10.05–12.94	1.03	Al <sub>2</sub> O <sub>3</sub> (synthetic)
Fe <sub>2</sub> O <sub>3</sub>	11.60	9.03–12.86	1.60	Fe <sub>2</sub> O <sub>3</sub> (synthetic)
SeO <sub>2</sub>	57.70	56.84–59.01	0.76	CdSe (synthetic)
H <sub>2</sub> O	19.14			Added in ideal value
Total*	99.83	99.70–100.08	0.13	

\*Bernardevansite is prone to the electron beam damage, however this did not seem to affect the relative proportions of cations. The large variations in the Al<sub>2</sub>O<sub>3</sub> and Fe<sub>2</sub>O<sub>3</sub> contents result from the strong correlation between the two components.  
S.D. – standard deviation

2022a), franksousaite PbCu(Se<sup>6+</sup>O<sub>4</sub>)(OH)<sub>2</sub> (Yang *et al.*, 2022b) and the new mineral bernardevansite, described herein.

#### Physical and chemical properties and Raman spectra

Bernardevansite occurs as aggregates or spheres of radiating bladed crystals (Figs 3,4,5) on a matrix consisting of Co-bearing krut'aitite–penroseite. Individual crystals of bernardevansite are found up to 0.10 × 0.03 × 0.01 mm, with elongation along [001] and common crystal forms {100}, {110},  $\bar{1}10$  and {001}. Bernardevansite is colourless in transmitted light and transparent with white streak, and has a vitreous lustre. It is brittle and has a Mohs hardness of 2½–3. Cleavage was not observed. The density measured by flotation in heavy liquids is 2.93(5) g/cm<sup>3</sup> and the calculated density is 2.997 g/cm<sup>3</sup> on the basis of the empirical chemical formula and unit-cell volume from single-crystal X-ray diffraction data. Optically, bernardevansite is biaxial (+), with  $\alpha = 1.642(5)$ ,  $\beta = 1.686(5)$ ,  $\gamma = 1.74(1)$  (determined in white light),  $2V$  (meas.) = 84(2)° and  $2V$  (calc.) = 87°. The pleochroism is very weak, from pale grey to grey, and dispersion was not observed. The calculated Gladstone-Dale compatibility index based on the empirical formula is 0.013 (superior) (Mandarino, 1981). Bernardevansite is insoluble in water or hydrochloric acid.

The chemical composition was determined using a Shimadzu-1720 electron microprobe (WDS mode, 15 kV, 10 nA and a beam diameter of 2 μm). The standards used for the probe analysis are given in Table 1, along with the determined compositions (11 analysis points). The resultant chemical formula, calculated on the basis of 15 O apfu (from the structure determination), is (Al<sub>1.26</sub>Fe<sub>0.82</sub><sup>3+</sup>)<sub>Σ2.08</sub>(Se<sub>0.98</sub>O<sub>3</sub>)<sub>3</sub>·6H<sub>2</sub>O, which can be simplified to (Al,Fe<sup>3+</sup>)<sub>2</sub>(SeO<sub>3</sub>)<sub>3</sub>·6H<sub>2</sub>O.

The Raman spectrum of bernardevansite (Fig. 6) was collected on a randomly oriented crystal with a Thermo Almega

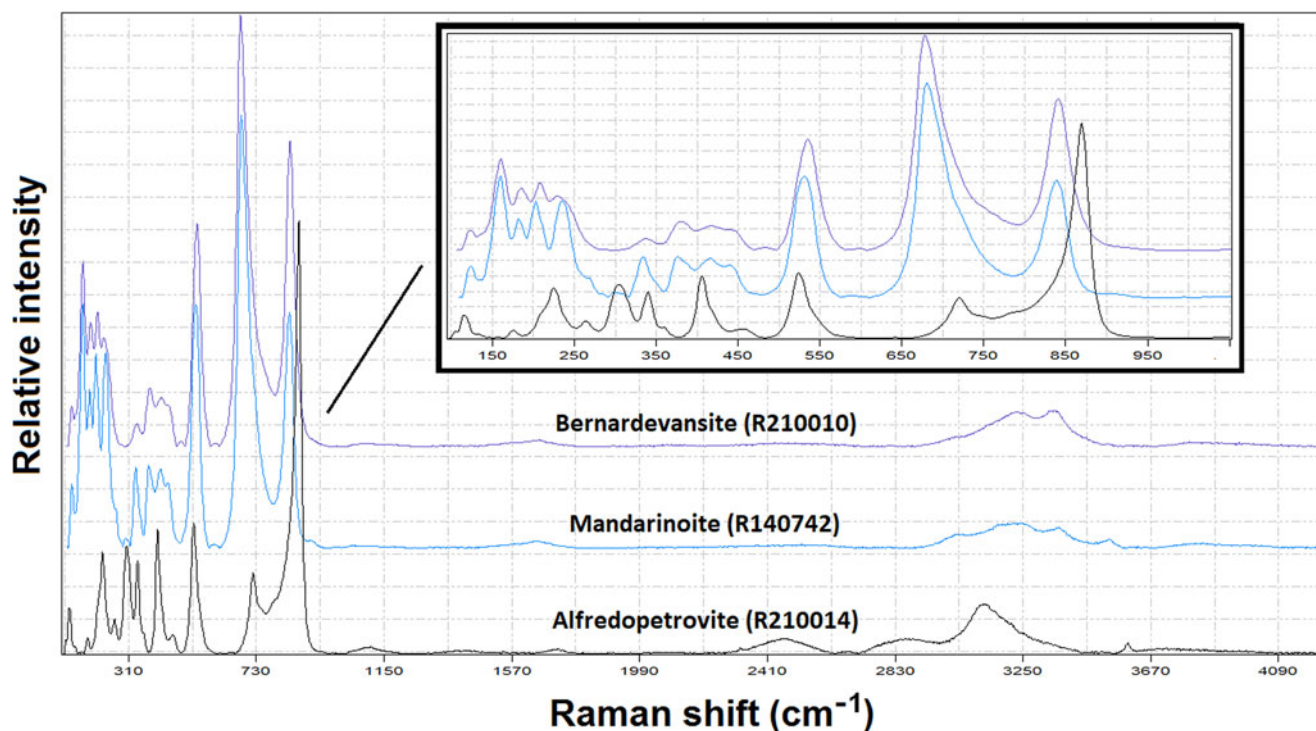


**Fig. 6.** Raman spectra of bernardevansite, mandarinoite and alfredopetrovite.

**Table 2.** Powder X-ray diffraction data (*d* in Å, *I* in %) for bernardevansite.\*

<i>l</i> <sub>cal</sub>	<i>l</i> <sub>meas</sub>	<i>d</i> <sub>meas</sub>	<i>d</i> <sub>calc</sub>	<i>hkl</i>	<i>l</i> <sub>cal</sub>	<i>l</i> <sub>meas</sub>	<i>d</i> <sub>meas</sub>	<i>d</i> <sub>calc</sub>	<i>hkl</i>
3.9	8	16.261	16.360	1 0 0	3.8	9	2.119	2.119	7 1 1
<b>37.1</b>	<b>39</b>	<b>8.147</b>	<b>8.180</b>	<b>2 0 0</b>	1.9	2	2.063	2.062	3 3 2
<b>100</b>	<b>100</b>	<b>7.036</b>	<b>7.023</b>	<b>1 1 0</b>	6.5	19	2.023	2.029	0 3 3
11	9	6.091	6.086	0 1 1	5	15	1.947	1.944	0 4 0
1.6	2	5.590	5.543	1 1 1	2.7	6	1.905	1.908	2 1 5
4.2	3	5.110	5.109	2 1 1	1.8	3	1.820	1.821	4 1 5
9.6	8	4.876	4.890	0 0 2	3	4	1.790	1.787	9 1 1
6.2	3	4.679	4.685	2 1 1	2.2	4	1.755	1.756	4 3 3
4.8	6	4.469	4.465	3 1 0	3	5	1.739	1.736	7 3 0
3	1	4.275	4.257	3 1 1	2.3	6	1.706	1.710	4 4 1
11.1	14	4.100	4.090	4 0 0	2.6	3	1.691	1.686	4 4 2
1.7	3	3.899	3.901	1 1 2	2.1	3	1.655	1.654	7 2 4
3.9	1	3.629	3.613	0 2 1	2.8	3	1.631	1.628	9 0 2
43	64	3.515	3.512	2 2 0	1.1	4	1.563	1.567	2 3 5
<b>26.6</b>	<b>47</b>	<b>3.385</b>	<b>3.388</b>	<b>4 0 2</b>	1.2	2	1.549	1.547	5 4 2
6.5	15	3.252	3.261	4 1 1	3.8	11	1.503	1.503	0 2 6
4.9	4	3.127	3.118	3 1 2	5.3	13	1.463	1.463	7 2 4
13.5	29	3.013	3.006	0 1 3	1.7	4	1.377	1.374	4 5 2
<b>31.7</b>	<b>80</b>	<b>2.943</b>	<b>2.940</b>	<b>2 2 2</b>	1.1	3	1.331	1.331	5 3 6
<b>17.2</b>	<b>37</b>	<b>2.769</b>	<b>2.772</b>	<b>2 2 2</b>	1.6	2	1.315	1.312	0 5 4
9.7	15	2.719	2.707	2 1 3	2.2	2	1.293	1.291	11 2 2
5.2	17	2.562	2.561	3 2 2	1.1	4	1.252	1.248	9 4 2
3	2	2.505	2.503	5 2 0	1.2	2	1.235	1.235	2 0 8
6.5	10	2.423	2.418	6 1 2					
2.6	5	2.356	2.355	1 1 4					
6.7	20	2.247	2.251	7 1 1					
6.1	10	2.172	2.165	3 3 2					

\*The strongest lines are given in bold

microRaman system, using a solid-state laser with a wavelength of 532 nm at 75 mW power and a thermoelectric cooled CCD detector. The laser is partially polarised with 4 cm<sup>-1</sup> resolution and a spot size of 1 μm.

### X-ray crystallography

Both the powder and single-crystal X-ray diffraction data for bernardevansite were collected on a Rigaku Xtalab Synerg D/S 4-circle diffractometer equipped with CuKα radiation. Powder

**Table 4.** Fractional atomic coordinates and equivalent isotropic displacement parameters (Å<sup>2</sup>) for bernardevansite.

Atom	<i>x/a</i>	<i>y/b</i>	<i>z/c</i>	<i>U</i> <sub>eq</sub>	Occ. (<1)
M1Al	0.39931(11)	0.74117(17)	0.9075(2)	0.0155(7)	0.692(14)
M1Fe	0.39931(11)	0.74117(17)	0.9075(2)	0.0155(7)	0.308(14)
M2Al	0.90506(9)	0.24015(16)	0.04690(19)	0.0141(6)	0.516(14)
M2Fe	0.90506(9)	0.24015(16)	0.04690(19)	0.0141(6)	0.484(14)
Se1	0.98068(4)	0.03893(9)	0.31646(7)	0.0160(2)	
Se2	0.22324(5)	0.72432(9)	0.72880(8)	0.0163(2)	
Se3	0.52831(4)	0.48070(9)	0.81382(7)	0.0164(2)	
O1	0.9810(3)	0.2129(7)	0.4212(6)	0.0205(10)	
O2	0.0775(3)	-0.0346(6)	0.3679(5)	0.0198(10)	
O3	0.9975(3)	0.1369(7)	0.1690(4)	0.0207(10)	
O4	0.3162(3)	-0.1799(6)	0.7648(5)	0.0200(10)	
O5	0.1905(3)	-0.1703(6)	0.5782(5)	0.0198(10)	
O6	0.1688(3)	-0.1636(6)	0.8314(5)	0.0219(10)	
O7	0.5208(3)	0.3791(7)	0.6612(5)	0.0216(10)	
O8	0.4297(3)	0.5494(6)	0.7990(5)	0.0182(10)	
O9	0.4774(3)	0.6800(6)	0.0686(5)	0.0196(10)	
O10	0.3191(3)	-0.4257(6)	0.9641(5)	0.0205(10)	
O11	0.3609(3)	-0.0850(6)	0.0260(5)	0.0240(10)	
O12	0.8865(3)	0.0117(6)	-0.0434(5)	0.0221(10)	
O13	0.6404(4)	0.7624(6)	0.0754(8)	0.0311(14)	
O14	0.2527(4)	0.3132(9)	0.1937(7)	0.0468(16)	
O15	0.1770(4)	0.2449(6)	0.4252(8)	0.0351(17)	

X-ray diffraction data were collected in the Gandolfi powder mode at 50 kV and 1 mA (Table 2) and the unit-cell parameters were refined using the program by Holland and Redfern (1997): *a* = 16.535(1), *b* = 7.7762(5), *c* = 9.8841(6) Å, β = 98.337(7)° and *V* = 1257.5(5) Å<sup>3</sup>.

All bernardevansite crystals examined are pervasively twinned on (100) with a twin law (1̄ 0 ½, 0 1̄ 0, 0 0 1). Single-crystal X-ray diffraction data were collected from a 0.03 × 0.02 × 0.01 mm fragment. The systematic absences of reflections suggest the unique space group *P*2<sub>1</sub>/*c*. The structure was solved and refined using *SHELX2018* (Sheldrick, 2015a, 2015b). No H atoms were located through the difference-Fourier syntheses. The refined Al/Fe ratios at the octahedral *M*1 and *M*2 sites are (0.692Al + 0.308Fe) and (0.516Al + 0.484Fe), respectively, yielding a total Al/Fe ratio of 1.208/0.792, which is very close to that (1.211/0.789, normalised)

**Table 3.** Summary of crystallographic data and refinement results for bernardevansite, mandarinoite and alfredopetrovite.

	Alfredopetrovite	Bernardevansite	Mandarinoite
Ideal formula	Al <sub>2</sub> (Se <sup>4+</sup> O <sub>3</sub> ) <sub>3</sub> ·6H <sub>2</sub> O	Al <sub>2</sub> (Se <sup>4+</sup> O <sub>3</sub> ) <sub>3</sub> ·6H <sub>2</sub> O	Fe <sub>2</sub> <sup>3+</sup> (Se <sup>4+</sup> O <sub>3</sub> ) <sub>3</sub> ·6H <sub>2</sub> O
Crystal symmetry	Hexagonal	Monoclinic	Monoclinic
Space group	<i>P</i> 6̄2 <i>c</i>	<i>P</i> 2 <sub>1</sub> / <i>c</i>	<i>P</i> 2 <sub>1</sub> / <i>c</i>
<i>a</i> (Å)	8.818(3)	16.5016(5)	16.810(4)
<i>b</i> (Å)	8.818(3)	7.7703(2)	7.880(2)
<i>c</i> (Å)	10.721(2)	9.8524(3)	10.019(2)
α (°)	90	90	90
β (°)	90	98.258(3)	98.26(2)
γ (°)	120	90	90
<i>V</i> (Å <sup>3</sup> )	722.0(5)	1250.21(6)	1310.4
<i>Z</i>	2	4	4
ρ <sub>cal</sub> (g/cm <sup>3</sup> )	2.50		2.98
2θ range for data collection (°)	≤40 (MoKα)	≤130.16 (CuKα)	≤60 (MoKα)
No. of reflections collected	1817	9235	4658
No. of independent reflections	246	3407	
No. of reflections with <i>I</i> > 2σ( <i>I</i> )	240	3156	2101
No. of parameters refined	40	184	
R(int)	0.064	0.037	
Final <i>R</i> <sub>1</sub> , <i>wR</i> <sub>2</sub> factors [ <i>I</i> > 2σ( <i>I</i> )]	0.027, 0.063	0.041, 0.110	0.064, 0.084
Goodness-of-fit	1.07	1.03	
Reference	Kampf et al. (2016a)	This study	Hawthorne (1984)

**Table 5.** Atomic displacement parameters ( $\text{\AA}^2$ ) for bernardevansite.

Atom	$U^{11}$	$U^{22}$	$U^{33}$	$U^{12}$	$U^{13}$	$U^{23}$
M1	0.0121 (10)	0.0190(10)	0.0155(11)	0.0002(5)	0.0025(7)	0.0015(5)
M2	0.0103(9)	0.0189(9)	0.0134(9)	-0.0004(5)	0.0031(6)	0.0008(4)
Se1	0.0132(4)	0.0198(4)	0.0149(4)	-0.0004(2)	0.0016(3)	0.0013(3)
Se2	0.0132(4)	0.0199(3)	0.0158(4)	-0.0005(3)	0.0023(3)	0.0006(3)
Se3	0.0135(4)	0.0198(4)	0.0160(4)	0.0002(3)	0.0022(3)	0.0008(3)
O1	0.015(2)	0.024(2)	0.024(3)	-0.002(2)	0.006(2)	-0.005(2)
O2	0.013(2)	0.021(2)	0.024(2)	0.0007(18)	-0.0010(19)	0.0049(19)
O3	0.015(2)	0.032(3)	0.015(2)	-0.002(2)	0.0026(17)	0.004(2)
O4	0.016(2)	0.026(3)	0.018(2)	-0.003(2)	0.0004(18)	0.000(2)
O5	0.015(2)	0.030(3)	0.015(2)	-0.002(2)	0.0039(18)	0.0007(19)
O6	0.017(2)	0.028(3)	0.021(2)	0.002(2)	0.0059(19)	0.001(2)
O7	0.018(2)	0.029(3)	0.017(2)	0.003(2)	0.0021(18)	-0.002(2)
O8	0.016(2)	0.022(2)	0.016(2)	0.0052(19)	0.0016(18)	0.0011(19)
O9	0.019(2)	0.022(2)	0.018(2)	0.002(2)	0.0017(18)	0.006(2)
O10	0.016(2)	0.022(2)	0.024(2)	0.003(2)	0.0044(19)	0.0028(19)
O11	0.027(3)	0.021(2)	0.023(2)	-0.002(2)	0.000(2)	0.003(2)
O12	0.018(2)	0.027(3)	0.022(2)	0.003(2)	0.006(2)	-0.002(2)
O13	0.027(3)	0.024(3)	0.043(4)	0.000(2)	0.010(3)	0.005(2)
O14	0.065(4)	0.036(4)	0.041(4)	0.007(3)	0.012(3)	0.003(3)
O15	0.023(3)	0.036(4)	0.047(4)	-0.006(2)	0.008(3)	-0.012(2)

measured from the electron microprobe analysis. The structure was refined as a 2-component twin with a twin ratio of 0.81/0.19. Final refinement statistics for bernardevansite are listed in Table 3. Atomic coordinates and displacement parameters are given in Tables 4 and 5, respectively. Selected bond distances are presented in Table 6. The bond-valence sums were calculated using the parameters given by Brese and O'Keeffe (1991) (Table 7). The crystallographic information file has been deposited with the Principal Editor of *Mineralogical Magazine* and is available as Supplementary material (see below).

### Crystal structure description and discussion

Bernardevansite,  $\text{Al}_2(\text{SeO}_3)_3 \cdot 6\text{H}_2\text{O}$ , is isostructural with mandarinoite,  $\text{Fe}_2^{3+}(\text{SeO}_3)_3 \cdot 6\text{H}_2\text{O}$  (Hawthorne, 1984), rather than with the Al end-member *P62c* alfredopetrovite,  $\text{Al}_2(\text{SeO}_3)_3 \cdot 6\text{H}_2\text{O}$  (Morris *et al.*, 1992; Kampf *et al.*, 2016a). In other words, it is

dimorphous with alfredopetrovite. The crystal structure of bernardevansite consists of a corner-sharing framework of  $M^{3+}\text{O}_6$  ( $M = \text{Al}$  and  $\text{Fe}$ ) octahedra and  $\text{Se}^{4+}\text{O}_3$  trigonal pyramids, leaving large voids that are occupied by the  $\text{H}_2\text{O}$  groups (Fig. 7). There are three unique Se positions in bernardevansite, each of which is coordinated to three O atoms to form characteristic  $\text{SeO}_3$  trigonal pyramids. There are two unique  $M^{3+}$  positions: M1 is octahedrally coordinated by (4O + 2 $\text{H}_2\text{O}$ ) and M2 by (5O +  $\text{H}_2\text{O}$ ). The structure refinement indicates that Al preferentially occupies M1 (= 0.692Al + 0.308Fe) over M2 (= 0.516Al + 0.484Fe). There are three distinct  $\text{H}_2\text{O}$  molecules (O13, O14 and O15) in the structure that are not bonded to any non-H cation (Table 7), in addition to three  $\text{H}_2\text{O}$  molecules (O10, O11 and O12) bonded to  $M$  cations. Although our structure determination failed to locate H atoms, all O–O distances for H-bonding in bernardevansite are consistent and comparable with those found in mandarinoite (Hawthorne, 1984) (Table 6).

**Table 6.** Selected bond distances ( $\text{\AA}$ ) for bernardevansite,  $\text{Al}_2(\text{SeO}_3)_3 \cdot 6\text{H}_2\text{O}$  and mandarinoite,  $\text{Fe}_2(\text{SeO}_3)_3 \cdot 6\text{H}_2\text{O}$ .\*

Ref:	Mandarinoite (1)	Bernardevansite (2)	Mandarinoite (1)	Bernardevansite (2)	Mandarinoite (1)	Bernardevansite (2)
M1–O4	1.980(11)	1.918(5)	Se1–O1	1.699(10)	O10–O5	2.629
M1–O7	1.956(12)	1.897(5)	Se1–O2	1.717(11)	O10–O13	2.768
M1–O8	2.007(10)	1.941(5)	Se1–O3	1.699(10)		
M1–O9	2.032(10)	1.954(5)	<Se1–O>	1.705	O11–O8	2.810
M1–O10	2.081(13)	1.989(5)			O11–O13	2.711
M1–O11	2.066(12)	1.950(5)	Se2–O4	1.699(11)		
<M1–O>	2.021	1.942	Se2–O5	1.728(11)	O12–O1	2.770
			Se2–O6	1.694(10)	O12–O3	2.886
M2–O1	1.967(10)	1.919(6)	<Se2–O>	1.707	O12–O15	2.709
M2–O2	2.011(11)	1.945(5)				
M2–O3	2.039(13)	1.973(5)	Se3–O7	1.698(9)	O13–O9	2.801
M2–O5	2.042(12)	1.983(5)	Se3–O8	1.710(10)	O13–O14	2.715
M2–O6	1.994(11)	1.923(5)	Se3–O9	1.717(10)		
M2–O12	2.074(12)	1.989(5)	<Se3–O>	1.708	O14–O15	2.815
<M2–O>	2.021	1.955			O14–O4	3.086
					O15–O2	2.729
					O15–O14	2.815
						2.732
						2.795

\*Notes:  $M = \text{Fe}$  and (Al,Fe) for mandarinoite and bernardevansite, respectively. References: (1) Hawthorne (1984); (2) this study.

**Table 7.** Bond-valence sums for bernardevansite.\*

	M1	M2	Se1	Se2	Se3	Sum
O1		0.544	1.348			1.892
O2		0.507	1.336			1.843
O3		0.470	1.358			1.828
O4	0.509			1.365		1.874
O5		0.458		1.305		1.763
O6		0.538		1.397		1.935
O7	0.539				1.397	1.936
O8	0.479				1.352	1.831
O9	0.463				1.295	1.758
O10	0.421					0.421
O11	0.468					0.468
O12		0.449				0.449
O13						-
O14						-
O15						-
Sum	2.878	2.967	4.042	4.068	4.044	

\*Note: The bond valence sums for M1 and M2 were calculated based on (0.692 Al + 0.308 Fe<sup>3+</sup>) and (0.516 Al + 0.484 Fe<sup>3+</sup>), respectively.

The substitution of the majority of Fe in mandarinoite by Al in bernardevansite results in a significant reduction in unit-cell volume from 1313.4 Å<sup>3</sup> to 1250.21(6) Å<sup>3</sup>, which motivated this investigation. Compared to mandarinoite, which has the identical average  $\langle M-O \rangle$  bond distances (2.021 Å) for the two octahedral sites (Hawthorne, 1984), the  $\langle M-O \rangle$  distance for the M1 site (1.942 Å) in bernardevansite is shorter than that for the M2 site (1.955 Å), consistent with the preference of Al at M1 over M2 (0.692 vs. 0.516), as the ionic radius of <sup>V</sup>Al<sup>3+</sup> (0.535 Å) is smaller than that of <sup>V</sup>Fe<sup>3+</sup> (0.645 Å) (Shannon, 1976). A survey of the literature appears to suggest that, for a structure with two

or more octahedral sites, Al<sup>3+</sup> is likely to be favoured by the site coordinated with more H<sub>2</sub>O molecules. This is indeed the case for bernardevansite, as the M1 site is coordinated by (4O + 2H<sub>2</sub>O) and M2 by (5O + H<sub>2</sub>O). Another typical example is coquimbite, which contains three distinct octahedral sites (M1, M2 and M3), with M1 coordinated by (6H<sub>2</sub>O), M2 by (6O<sup>2-</sup>) and M3 by (3H<sub>2</sub>O + 3O<sup>2-</sup>). All structure determinations on coquimbite have shown that Al<sup>3+</sup> is predominately or exclusively ordered into the M1 site (e.g. Demartin *et al.*, 2010; Yang and Giester, 2018; Mauro *et al.*, 2020 and references therein).

According to the Raman spectroscopic studies on hydrous materials containing (SeO<sub>3</sub>)<sup>2-</sup> (e.g. Wickleder *et al.*, 2004; Frost *et al.*, 2006; Frost and Keeffe, 2008; Djemel *et al.*, 2013; Wolak *et al.*, 2013; Kasatkin *et al.*, 2014; Mills *et al.*, 2014; Kampf *et al.*, 2016b), we made the following tentative assignments of major Raman bands for bernardevansite. The broad bands between 2900 and 3500 cm<sup>-1</sup> and those between 1500 and 1750 cm<sup>-1</sup> are due to the O–H stretching and H–O–H bending modes in H<sub>2</sub>O groups, respectively. The bands at 844 and 685 cm<sup>-1</sup> are ascribable to the Se<sup>4+</sup>–O symmetric and antisymmetric stretching vibrations, respectively, within the Se<sup>4+</sup>O<sub>3</sub> groups, whereas those from 320 to 570 cm<sup>-1</sup> originate from the O–Se<sup>4+</sup>–O bending modes. The bands below 320 cm<sup>-1</sup> are mainly associated with the rotational and translational modes of Se<sup>4+</sup>O<sub>3</sub> groups, as well as the M<sup>3+</sup>–O interactions and lattice vibrational modes.

For comparison, the Raman spectra of alfredopetrovite, Al<sub>2</sub>(Se<sup>4+</sup>O<sub>3</sub>)<sub>3</sub>·6H<sub>2</sub>O and mandarinoite, Fe<sub>2</sub><sup>3+</sup>(Se<sup>4+</sup>O<sub>3</sub>)<sub>3</sub>·6H<sub>2</sub>O, from the RRUFF Project (<http://rruff.info/R210014> and <http://rruff.info/R140742>, respectively) are also plotted in Fig. 6. Evidently, the spectrum of bernardevansite is more similar to that of

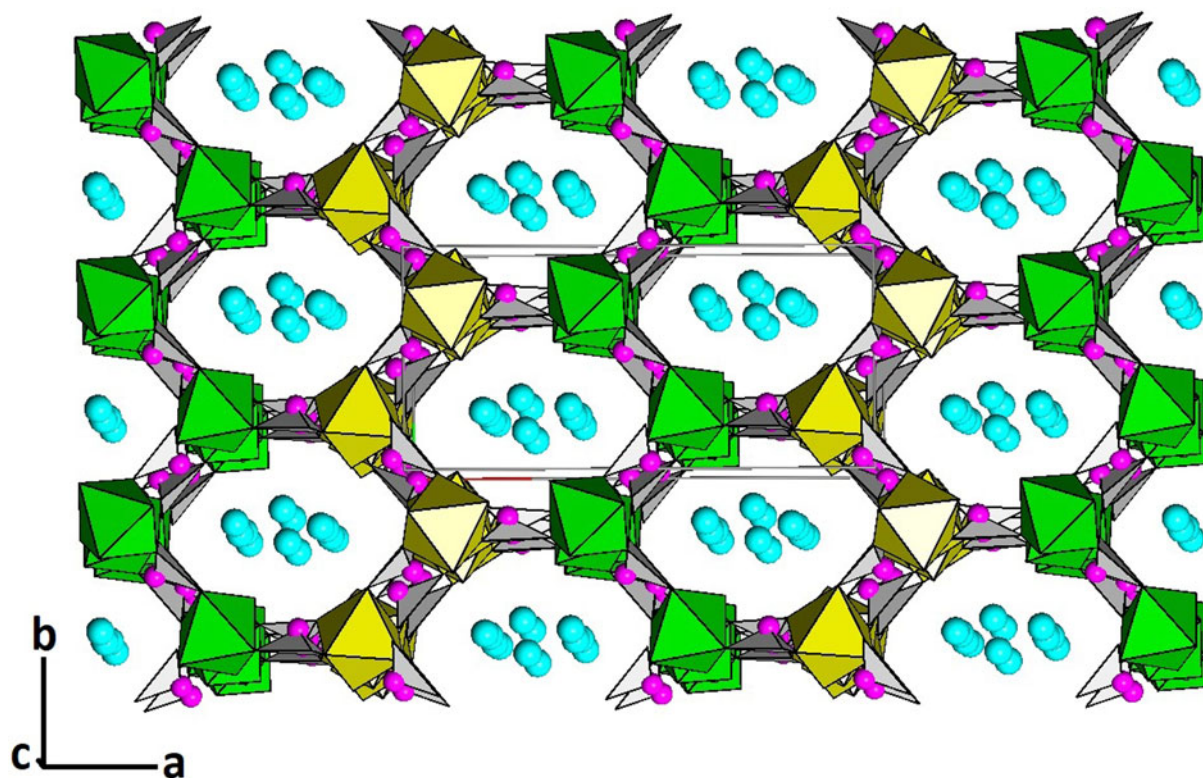


**Fig. 7.** Crystal structure of bernardevansite. Green, yellow and grey polyhedra represent M1O<sub>6</sub>, M2O<sub>6</sub> and SeO<sub>3</sub> groups, respectively. Purple and aqua spheres represent Se (Se1, Se2 and Se3) atoms and H<sub>2</sub>O (O13, O14 and O15) groups that are not bonded to any non-H cation, respectively.

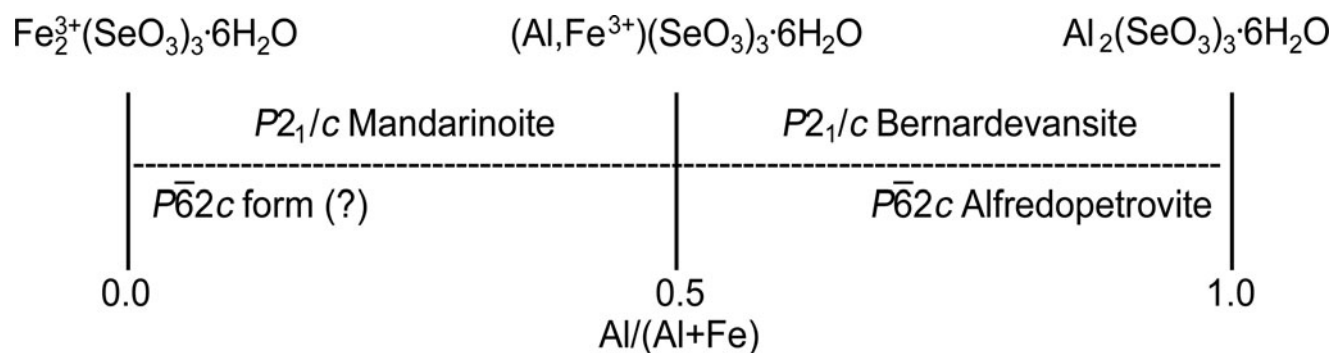


Fig. 8. A concept of classification of  $M^{3+}(\text{SeO}_3)_3 \cdot 6\text{H}_2\text{O}$  minerals ( $M = \text{Al}$  and  $\text{Fe}$ ).

mandarinoite than to that of alfredopetrovite, pointing to the structural similarities between bernardevansite and mandarinoite.

Although the bernardevansite sample we studied here,  $(\text{Al}_{0.61}\text{Fe}_{0.39})_2(\text{SeO}_3)_3 \cdot 6\text{H}_2\text{O}$ , is isostructural with mandarinoite, its chemistry is closer to that of alfredopetrovite, the Al end-member of the  $\text{Fe}_2^{3+}(\text{SeO}_3)_3 \cdot 6\text{H}_2\text{O} - \text{Al}_2(\text{SeO}_3)_3 \cdot 6\text{H}_2\text{O}$  system, as illustrated in Fig. 8. This raises an interesting question about its ideal chemical formula. Should it be expressed as (1) an Fe-bearing formula,  $(\text{Al}_{1-x}\text{Fe}_x)_2(\text{SeO}_3)_3 \cdot 6\text{H}_2\text{O}$ , where  $0 < x < 0.5$ , or (2) an Fe-free end-member formula,  $\text{Al}_2(\text{SeO}_3)_3 \cdot 6\text{H}_2\text{O}$ . The first Fe-bearing formula requires that Fe is essential to stabilise the  $P2_1/c$  mandarinoite-type structure and there is no complete solid-solution series between  $\text{Al}_2(\text{SeO}_3)_3 \cdot 6\text{H}_2\text{O}$  and  $\text{Fe}_2(\text{SeO}_3)_3 \cdot 6\text{H}_2\text{O}$ . This formula appears to be consistent with synthetic experiments, as several hydrothermal syntheses of Al selenites conducted thus far have revealed only the hexagonal form of  $\text{Al}_2(\text{SeO}_3)_3 \cdot 6\text{H}_2\text{O}$  and no monoclinic form (Morris *et al.*, 1992; Ratheesh *et al.*, 1997 and references therein). In contrast, the second Fe-free formula implies that  $\text{Al}_2(\text{SeO}_3)_3 \cdot 6\text{H}_2\text{O}$  possesses two polymorphs: a monoclinic  $P2_1/c$  mandarinoite-type form and a hexagonal  $P6_2c$  alfredopetrovite form. Regardless of its ideal chemical formula, the discovery of bernardevansite begs the question whether the  $\text{Fe}^{3+}$  end-member,  $\text{Fe}_2^{3+}(\text{SeO}_3)_3 \cdot 6\text{H}_2\text{O}$ , has two polymorphs as well, one with  $P2_1/c$  symmetry, as for mandarinoite, and the other  $P6_2c$ , as for alfredopetrovite.

**Acknowledgements.** We are grateful for the constructive comments by Drs Anthony Kampf and Peter Leverett. This study was funded by the Feinglos family and Mr. Michael M. Scott.

**Supplementary material.** To view supplementary material for this article, please visit <https://doi.org/10.1180/mgm.2023.7>

**Competing interests.** The authors declare none.

## References

- Brese N.E. and O'Keeffe M. (1991) Bond-valence parameters for solids. *Acta Crystallographica*, **B47**, 192–197.
- Demartin F., Castellano C., Gramaccioli C.M. and Campostrini I. (2010) Aluminum-for-iron substitution, hydrogen bonding, and a novel structure-type in coquimbite-like minerals. *The Canadian Mineralogist*, **48**, 323–333.
- Djemel M., Abdelhedi M., Ktari L. and Dammak M. (2013) X-ray diffraction, Raman study and electrical properties of the new mixed compound  $\text{Rb}_{1.7}\text{K}_{0.3}(\text{SO}_4)_{0.88}(\text{SeO}_4)_{0.12}\text{Te}(\text{OH})_6$ . *Journal of Molecular Structure*, **1047**, 15–21.
- Förster H.-J., Bindi L. and Stanley C.J. (2016) Grundmannite,  $\text{CuBiSe}_2$ , the Se-analogue of emplectite, a new mineral from the El Dragón mine, Potosí, Bolivia. *European Journal of Mineralogy*, **28**, 467–477.
- Förster H.-J., Bindi L., Stanley C.J. and Grundmann G. (2017) Hansblockite,  $(\text{Cu,Hg})(\text{Bi,Pb})\text{Se}_2$ , the monoclinic polymorph of grundmannite: a new mineral from the Se mineralization at El Dragón (Bolivia). *Mineralogical Magazine*, **81**, 229–240.
- Förster H.-J., Bindi L., Grundmann G. and Stanley C.J. (2018) Cerramojonite,  $\text{CuPbBiSe}_3$ , from El Dragón (Bolivia): A new member of the bournonite group. *Minerals*, **8**, 420.
- Förster H.-J., Ma C., Grundmann G., Bindi L. and Stanley C.J. (2019) Nickelytyrellite,  $\text{CuNi}_2\text{Se}_4$ , a new member of the spinel supergroup from El Dragón, Bolivia. *The Canadian Mineralogist*, **57**, 637–646.
- Frost R.L. and Keeffe E.C. (2008) Raman spectroscopic study of the schmierite  $\text{Pb}_2\text{Cu}_2[(\text{OH})_4|\text{SeO}_3|\text{SeO}_4]$ . *Journal of Raman Spectroscopy*, **39**, 1408–1402.
- Frost R.L., Weier M.L., Reddy B.J. and Čejka J. (2006) A Raman spectroscopic study of the uranyl selenite mineral haynesite. *Journal of Raman Spectroscopy*, **37**, 816–821.
- Grundmann G. and Förster H.-J. (2017) Origin of the El Dragón Selenium Mineralization, Quijarro Province, Potosí, Bolivia. *Minerals*, **7**, 1–68.
- Grundmann G., Lehrberger G. and Schnorrer-Köhler G. (1990) The El Dragón mine, Potosí, Bolivia. *Mineralogical Record*, **21**, 133–150.
- Grundmann G., Lehrberger G. and Schnorrer-Köhler G. (2007) The “El Dragón Mine”, Porco, Potosí, Bolivia - Selenium minerals. *Mineral UP*, **1**, 16–25.
- Hawthorne F.C. (1984) The crystal structure of mandarinoite,  $\text{Fe}_2^{3+}\text{Se}_3 \cdot 6\text{H}_2\text{O}$ . *The Canadian Mineralogist*, **22**, 475–480.
- Holland T.J.B. and Redfern S.A.T. (1997) Unit cell refinement from powder diffraction data: the use of regression diagnostics. *Mineralogical Magazine*, **61**, 65–77.
- Kampf A.R., Mills S.J., Nash B.P., Thorne B. and Favreau G. (2016a) Alfredopetrovite, a new selenite mineral from the El Dragón mine, Bolivia. *European Journal of Mineralogy*, **28**, 479–484.
- Kampf A.R., Mills S.J. and Nash B.P. (2016b) Pauladamsite,  $\text{Cu}_4(\text{SeO}_3)(\text{SO}_4)(\text{OH})_4 \cdot 2\text{H}_2\text{O}$ , a new mineral from the Santa Rosa mine, Darwin district, California, USA. *Mineralogical Magazine*, **80**, 949–958.
- Kasatkin A.V., Plášil J., Marty J., Agakhanov A.A., Belakovskiy D.I. and Lykova I.S. (2014) Nestolaite,  $\text{CaSeO}_3 \cdot \text{H}_2\text{O}$ , a new mineral from the Little Eva mine, Grand County, Utah, USA. *Mineralogical Magazine*, **78**, 497–505.
- Mandarino J.A. (1981) The Gladstone–Dale relationship. IV. The compatibility concept and its application. *The Canadian Mineralogist*, **19**, 441–450.
- Mauro D., Biagioni C., Pasero M., Skogby H. and Zaccarini F. (2020) Redefinition of coquimbite,  $\text{AlFe}_3^{3+}(\text{SO}_4)_6(\text{H}_2\text{O})_{12} \cdot 6\text{H}_2\text{O}$ . *Mineralogical Magazine*, **84**, 275–282.
- Mills S.J., Kampf A.R., Housley R.M., Christy A.G., Thorne B., Chen Y.-S. and Steele I.M. (2014) Favreaite, a new selenite mineral from the El Dragón mine, Bolivia. *European Journal of Mineralogy*, **26**, 771–781.
- Morris R.E., Harrison W.T.A., Stucky G.D. and Cheetham A.K. (1992) On the structure of  $\text{Al}_2(\text{SeO}_3)_3 \cdot 6\text{H}_2\text{O}$ . *Journal of Solid State Chemistry*, **99**, 200.
- Paar W.H., Cooper M.A., Moëlo Y., Stanley C.J., Putz H., Topa D., Roberts A.C., Stirling J., Raith J.G. and Rowe R. (2012) Eldragónite,

- Cu<sub>6</sub>BiSe<sub>4</sub>(Se<sub>2</sub>), A new mineral species from the El Dragón Mine, Potosí, Bolivia, and its crystal structure. *The Canadian Mineralogist*, **50**, 281–294.
- Ratheesh R., Suresh G., Nayar V.U. and Morris R.E. (1997) Vibrational spectra of three aluminum selenities Al<sub>2</sub>(SeO<sub>3</sub>)<sub>3</sub>·3H<sub>2</sub>O, Al<sub>2</sub>(SeO<sub>3</sub>)<sub>3</sub>·6H<sub>2</sub>O and AlH(SeO<sub>3</sub>)<sub>2</sub>·H<sub>2</sub>O. *Spectrochimica Acta Part A: Molecular and Biomolecular Spectroscopy*, **53**, 1975–1979.
- Shannon R.D. (1976) Revised effective ionic radii and systematic studies of interatomic distances in halides and chalcogenides. *Acta Crystallographica*, **A32**, 751–767.
- Sheldrick G.M. (2015a) SHELXT – Integrated space-group and crystal structure determination. *Acta Crystallographica*, **A71**, 3–8.
- Sheldrick G.M. (2015b) Crystal structure refinement with SHELX. *Acta Crystallographica*, **C71**, 3–8.
- Wickleder M.S., Buchner O., Wickleder C., Sheik S.E., Brunklaus G. and Eckert H. (2004) Au<sub>2</sub>(SeO<sub>3</sub>)<sub>2</sub>(SeO<sub>4</sub>): Synthesis and characterization of a new non-centrosymmetric selenite-selenate. *Inorganic Chemistry*, **43**, 5860–5864.
- Wolak J., Pawlowski A., Polomska M. and Pietraszko A. (2013) Molecular dynamics in (NH<sub>4</sub>)<sub>3</sub>H(SeO<sub>4</sub>)<sub>2</sub> at superionic phase transitions: Raman spectroscopy study. *Phase Transitions*, **86**, 182–190.
- Yang Z. and Giester G. (2018) Structure refinements of coquimbite and para-coquimbite from the Hongshan Cu–Au deposit, NW China. *European Journal of Mineralogy*, **30**, 849–858.
- Yang H., Gu X., Jenkins R.A., Gibbs R.B., McGlasson J.A. and Scott M.M. (2022a) Petermegawite, IMA2021-079. CNMNC Newsletter 64. *Mineralogical Magazine*, **86**, 178–182, <https://doi.org/10.1180/mgm.2021.93>.
- Yang H., McGlasson J.A., Gibbs R.B. and Downs R.T. (2022b) Franksousaite, PbCu(Se<sup>6+</sup>O<sub>4</sub>)(OH)<sub>2</sub>, the Se<sup>6+</sup> analogue of linarite, a new mineral from the El Dragón mine, Potosí, Bolivia. *Mineralogical Magazine*, **86**, 792–798.
- Yang H., Gu X., Jenkins R.A., Gibbs R.G. and Downs R.T. (2023) Bernardevansite, IMA 2022-057. CNMNC Newsletter 70, *Mineralogical Magazine*, **87**, 160–168, <https://doi.org/10.1180/mgm.2022.135>